Modified zinc oxide nanoparticles as potential drug carrier

J. Pulit-Prociak[a],[*], A. Staroń[a], D. Domagała[b], J. Kojs[c], M. Zielina[d], M. Banach[a]
[a]*Faculty of Chemical Engineering and Technology, Institute of Chemistry and Inorganic Technology, Cracow University of Technology, Warszawska 24, Cracow 31-155, Poland*
[b]*Department of Human Nutrition and Dietetics, Faculty of Food Technology, University of Agriculture in Krakow, Balicka 122, Cracow 30-149, Poland*
[c]*Gabriel Narutowicz Specialist City Hospital, Neurology Ward and Stroke Ward, Prądnicka 35-37, 31-202 Cracow, Poland*
[d]*Faculty of Environmental Engineering and Energy, Cracow University of Technology, Warszawska 24, Cracow 31-155, Poland*

The objective of this research was to investigate the feasibility of creating a stable drug carrier using zinc oxide. This carrier, with its surface modified by a galactose coating, aimed to demonstrate reduced toxicity compared to the uncoated zinc oxide nanoparticles. A series of zinc oxide nanoparticles were synthesized, each modified with galactose. The processes were carried out in a microwave radiation field. The synthesized products underwent analysis, including XRD, ATR-FTIR and TEM-EDS analysis. Also, DLS technique was applied to determined size and electrokinetic potential of nanoparticles in different media. Further investigation assessed the impact of the synthesized zinc oxide nanoparticles on CHO cell cytotoxicity and their proliferation. XRD technique confirmed the obtaining of zinc oxide nanoparticles. Modification with galactose didn't impact their purity. ATR-FTIR analysis confirmed Zn-O bonds. Galactose presence was confirmed at its highest molar ratio. TEM-EDS analysis revealed pure zinc oxide nanoparticles' spiked structure and modified nanoparticles' less organized arrangement, both showing bar-like shape. DLS technique determined nanoparticle sizes between 217 and 764 nm. Nanoparticle suspensions were found stable in various environments. In vitro cell viability analysis indicated reduced cytotoxicity and enhanced cell development with modified zinc oxide nanoparticles compared to reference unmodified particles. Regarding the outcomes, it can be deduced that the suggested process parameter values consistently yield stable galactose-modified zinc oxide nanoparticles. These modified nanoparticles exhibit lower cytotoxicity towards CHO cells compared to pure zinc oxide. Furthermore, they actively promote the proliferation of normal cells, aligning with the desired outcome.

(Received November 3, 2023; Accepted April 13, 2024)

Keywords: Zinc oxide, Nanoparticles, Galactose

1. Introduction

Nanotechnology stands as a burgeoning scientific realm that presents novel prospects across numerous facets of life. This emanates from the distinguishing factor that in nanomaterials, the proportion of surface atoms to those within the particle's core is substantially high. Consequently, their physicochemical traits deviate markedly from those exhibited by macro-scale materials [1-3]. Nanomaterials are defined by at least one dimension measuring below 100 nm. This dimensionality alteration induces shifts in the behavior of these materials under external forces, resulting in heightened biological and chemical reactivity, as well as amplified optical and electrical properties [4,5]. The spectrum of nanomaterials encompasses point-like structures, nanoplatelets, multilayer constructs, nanotubes, nanowires, and nanoparticles, which encapsulate nanocrystalline forms [6]. Owing to the inherently interdisciplinary nature of nanotechnology,

[*] Corresponding author: jolanta.pulit-prociak@pk.edu.pl
https://doi.org/10.15251/DJNB.2024.192.581

these nanomaterials find utility across diverse domains, including materials engineering, electronics, environmental conservation, pharmaceuticals, cosmetics, and medicine [7,8].

The utilization of nanomaterials as carriers for drug delivery has garnered significant attention [9-11], primarily to facilitate the development of precision therapies and the controlled administration of medications. The chosen carrier must not possess toxic attributes, but rather form a stable binding with the drug. This binding should enable targeted delivery and controlled release at a specific site with the appropriate dosage. The therapeutic efficacy of nanoparticles is notably remarkable due to the ability to tailor their retention duration, solubility, and ability to penetrate biological barriers. This holds particular significance for patients as it enhances treatment effectiveness while concurrently mitigating therapy-related side effects [12–14]. Conjugates incorporating nanoparticles can be guided using targeting agents like folic acid, peptides, or saccharides [15]. Nanocapsulation yields an augmented therapeutic index for the encapsulated active components and introduces alterations in drug distribution patterns. In cases where particle cores are composed of metallic materials, coatings are intricately designed to shield them from environmental-induced alterations [16,17].

The process of targeted transport can occur through passive or active mechanisms. In the former scenario, heightened permeability of capillary endothelial cells transpires at the tumor site, while in the latter, targeting ligands attach to receptors situated within the affected tissue [16,18,19]. Zinc oxide stands as a compelling contender for targeted anticancer therapies due to its augmented retention, permeability, and specific cytotoxicity [20]. Regarding practical implementation, metal nanoparticles within the 10 to 100 nm size range offer optimal benefits, as they penetrate healthy tissues to a limited extent while interacting with diseased tissues. Nanoparticles measuring less than 10 nm infiltrate deeper into tumors, albeit potentially exerting a toxic impact on healthy tissue [21,22].

Surface functionalization of nanoparticles holds the promise of enhancing anti-cancer therapies by enabling efficient penetration of plasma membranes and precise localization [23,24]. In vitro investigations have substantiated the cytotoxic effects of metal nanoxides, such as zinc nanoxide, on various cancer cell lines including human brain and cervical glioma cells, hepatocellular carcinoma cells, and bladder cancer cells [25–30]. Animal model-based research has demonstrated the proficient eradication of cancer cells by nanoscale zinc oxide, while leaving astrocytes and hepatocytes unaffected. This observation underscores the substantial potential of zinc oxide nanoparticles in the realm of oncological applications [27].

The aim of this study was to check whether there is a possibility to obtain a stable zinc oxide based drug carrier which thanks to its surface modification by galactose coating would be less toxic comparing to the bare zinc oxide nanoparticles.

2. Experimental

2.1. Materials

In the processes of formation modified zinc oxide nanoparticles the following compounds were used in this study: zinc nitrate (99.0%), sodium hydroxide (≥98.-%) and D-(+)-galactose (≥99.0%). All compounds were obtained from Sigma-Aldrich. All aqueous solutions were prepared using deionized water (Polwater, 0.18 μS). CHO cell line, culture media (F-12K Medium) and supplements (FBS, antibiotics) were obtained from Sigma-Aldrich. LDH cytotoxicity assay Kit was obtained from Thermo Fisher Scientific and BrdU cell proliferation kit was obtained from Roche.

2.2. Methods

A series of nine zinc oxide nanoparticles modified with galactose was obtained based on the precipitation and dehydration processes. Dehydration process was performed in microwave reactor, Magnum II, Ertec Poland. In the role of zinc ions source, zinc nitrate was used. Sodium hydroxide served as precipitating agent. In order to modify the surface of zinc oxide nanoparticles, D-(+)-galactose was used. The design of experiment assumed obtaining nine products which varied in values of process parameters of their production. The group of input (independent)

parameters included the molar ratio of galactose to theoretical mass of produced zinc oxide, fold of NaOH vs. stoichiometric amount and temperature of the microwave process. The schematic diagram of the process is presented in Figure 1. All concentrations and volumes of the individual chemicals were also calculated as the theoretical final weight of zinc oxide was equal to 1.01725 g (0.0125 mole). Briefly, the aqueous sodium hydroxide solution was added dropwise to the aqueous solution of zinc nitrate which was in a 100 ml Teflon vessel. In the reaction of precipitation process, zinc hydroxide was formed. The obtained suspension was homogenized for 60 seconds (Hielscher UP400St, 40W). In the next step the aqueous solution of galactose was introduced into the mixture and the whole was homogenized again for additional 60 seconds. Later on the Teflon vessel was placed in the chamber of Magnum II microwave reactor (Ertec Poland) in which the zinc hydroxide dehydration process was completed. The process temperature was set according to the design of experiment and the process time (after reaching this required temperature) was equal to 5 minutes. The obtained mixture was filtered and the solid residue was washed with deionized water twice. The filtrate was discarded and the solid product was dried in a laboratory drier at 80˚C for 24 h. The dried products have been grinded in an agate mortar. The specific values of input parameters are provided in Table 1.

Table 1. Process parameters.

Sample	**Input parameters**		
	n GAL : n ZnO	**fold of NaOH vs. stoichiometric amount**	**process temperature, °C**
F1	0.02	1	120
F2	0.02	2	180
F3	0.02	3	150
F4	0.11	1	180
F5	0.11	2	150
F6	0.11	3	120
F7	0.20	1	150
F8	0.20	2	120
F9	0.20	3	180
F/Base	0	1	150

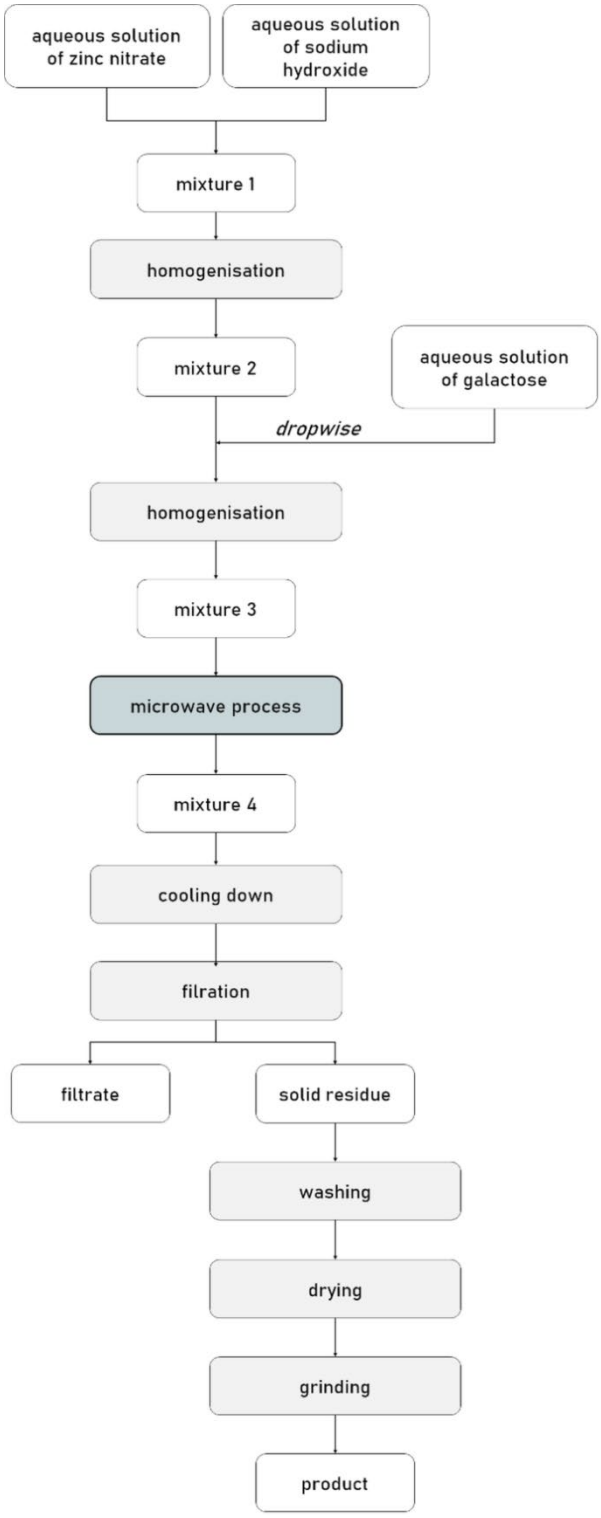

Fig. 1. Schematic diagram of the process.

A reference product without galactose was also prepared. This material was obtained with the stoichiometric amount of required sodium hydroxide and in 150°C. The obtained products were analysed. The crystallographic structure of zinc oxide was assessed by XRD technique (X'Pert PW 1752/00, Philips). Based on Scherrer equation the crystalline size was calculated. The confirmation of the organic matter on the surface of zinc oxide nanoparticles was performed in the course of ATR-FTIR analysis (Nicolet 380 spectrophotometer, Thermo Fisher). The step was

taken in order to confirm indirectly the incorporation of galactose. TEM-EDS microscopy was applied in order to assess the size and shape of nanoparticles (Tecnai TEM G2 F20X-Twin 200 kV, FEI). Size and electrokinetic potential of zinc oxide nanoparticles suspended in different medium (aqueous, Ringer fluid and SBF (simulated body fluid)) at a concentration of 10 ppm was assessed by applying DLS technique (Zetasizer Nano ZS, Malvern Instruments Ltd). Before this analysis the suspensions have been homogenized for 1 minute.

2.2.1. In Vitro Cell viability assay

Subsequent investigation delved into the impact of the synthesized zinc oxide nanoparticles on the cytotoxicity and proliferation of Chinese hamster ovary (CHO) cells. For this assessment, CHO cells (Sigma-Aldrich, catalog no. 85051005) were utilized, cultivated in accordance with the manufacturer's guidelines. The cells were nurtured in F-12K medium (Sigma-Aldrich, catalog no. N4888), supplemented with fetal bovine serum (Thermo Fisher Scientific, catalog no. 10270106), and antibiotics (Sigma-Aldrich, catalog no. P4333). The cell cultures were maintained at a temperature of 37°C with a 5% CO2 environment, and cell passaging occurred when the confluence reached 80%, approximately 2-3 times per week. The lactate dehydrogenase (LDH) assay stands as a colorimetric technique employed to assess the cytotoxic impact of test substances on cells. This assay quantifies the production of colored formazan (measured for absorbance at 490 nm) resulting from the conversion of tertazoline. This conversion is facilitated by the enzyme lactate dehydrogenase in the presence of NAD+. The breakdown of cell membrane integrity leads to the release of lactate dehydrogenase from deceased cells into the culture medium.

For the cytotoxicity evaluation, CHO cells were plated into 96-well plates at a density of 9×10^3 cells per well in a volume of 150 µL of medium. Following a 24-hour stabilization period, the medium was substituted with fresh medium containing varying concentrations of nanomaterials (80, 70, 50, 30, and 10 µg/mL), and a control without nanoparticles. Cytotoxicity analysis of the nanomaterials was conducted utilizing the Pierce LDH cytotoxicity kit (Thermo Fisher Scientific, Cat. No. 88954) in accordance with the manufacturer's provided protocol. Measurements were taken using a Multiskan GO microplate reader (Thermo Fisher Scientific) at two wavelengths: 490 nm (for formazan absorbance) and 680 nm (for background absorbance). The cytotoxicity was determined through the following equations (1):

$$\%\ \text{Cytotoxicity} = \frac{\text{Compound-treated LDH activity} - \text{Spontaneous LDH activity}}{\text{Maximum LDH activity} - \text{Spontaneous LDH activity}} \cdot 100 \quad (1)$$

The BrdU proliferation analysis assay employs a colorimetric approach to quantify the incorporation of 5-bromo-2'-deoxyuridine (BrdU) into DNA. BrdU, a synthetic analogue of thymidine nucleoside, integrates into the DNA of actively dividing cells during the S phase of the cell cycle. The quantity of integrated BrdU is determined through an enzymatic reaction involving an enzyme conjugated with an anti-BrdU antibody and a substrate. This reaction takes place within previously fixed cells. A strong signal indicates heightened cellular proliferation activity, whereas a weak signal suggests an inhibition of cell division.

For the proliferation analysis, CHO cells were seeded into 96-well plates at a density of 9×10^3 cells per well in a volume of 150 µL of medium. After a 24-hour stabilization period, the medium was substituted with fresh medium containing nanomaterials, along with a nanoparticle-free control. The cells were then cultured for 24, 48, and 72 hours. The evaluation of cell proliferation in the presence of nanomaterials was executed using the Cell Proliferation ELISA kit, BrdU (Roche, Cat # 11647229001), following the manufacturer's protocol. Measurements were taken using a Multiskan GO microplate reader (Thermo Fisher Scientific) at two wavelengths: 450 nm (for product absorbance) and 690 nm (for background absorbance).

3. Results

The XRD spectra of all prepared products are presented in Figure 2A. One may observe that the diffractograms of pure zinc oxide and modified products do not differ from each other.

There peaks which are characteristic for zinc oxide are noted at 31.7, 34.4, 36.3, 47.4 and 56.5°. Any other peaks have not been found which confirms obtaining of pure zinc oxide in the products. The purity of the obtained products is not affected by the modification of the products with galactose and tannic acid.

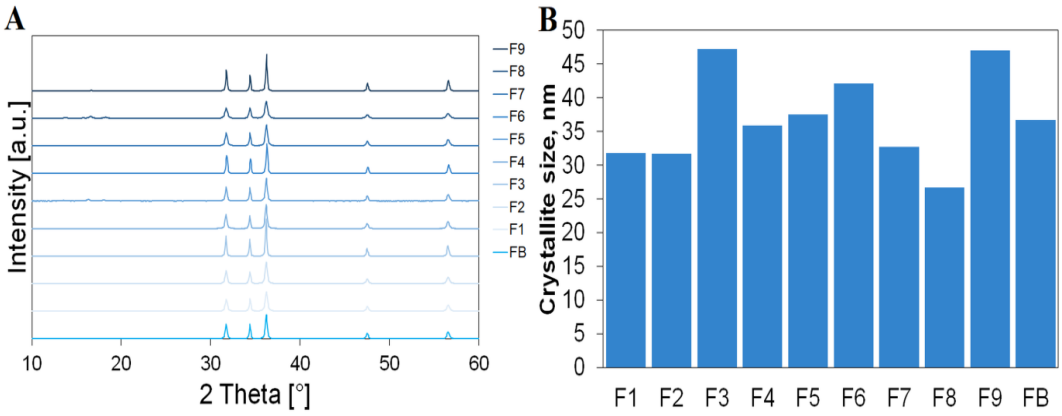

Fig. 2. A) XRD diffractograms of all obtained products, B) Crystallite size calculated based on Scherrer equation.

The XRD peaks width has been taken in order to perform the analysis of crystallite size. The crystallite size was calculated based on Scherrer's formulae, which is:

$$d_{Sch}=k\lambda/\beta\cos\theta$$

where the constant k depends on the shape of the crystallite size, β is the width at half maximum peak describing the material, λ is the wavelength of CuKa radiation, θ is the Bragg diffraction angle and d_{Sch} is the crystallite size. Its results are presented in Figure 2B. The range of crystallite size is between 26.7 and 47.2 nm. The crystallite size of modified products did not differ from the size of crystallites of reference, bare zinc oxide nanoparticles.

The prepared materials have been analysed by ATR-FTIR spectroscopy. The results of this analysis have been shown in Figure 3. The bonds of Zn-O have been confirmed by strong peaks around 490 cm^{-1}. Weak peaks near 3380 cm^{-1} correspond to the hydroxyl group of adsorbed water. Peaks around 2330 cm^{-1} are from atmospheric CO_2. The presence of gallactose has been confirmed in samples with the highest amount of this modifying compound (samples F7, F8 and F9 in which the molar ratio of galactose to zinc oxide nanoparticles was equal to 0.2).

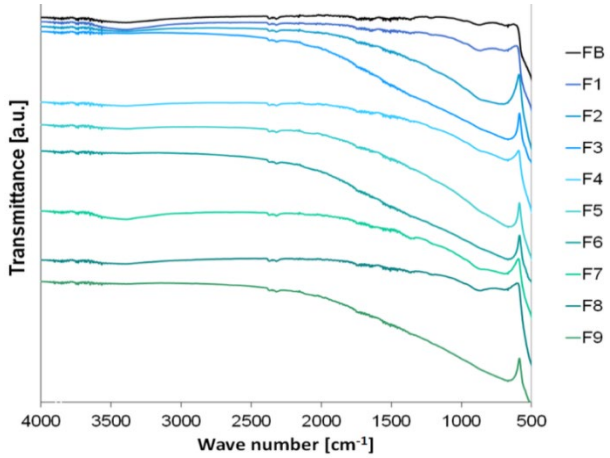

Fig. 3. ATR-FTIR spectra of obtained materials.

The peaks at 849, 1363 and 1695 cm^{-1} are characteristic for C-C, C-O and C = O bonds. What is more, peaks at 1363 cm^{-1} origins from CH_2 group present in galactose.

Figure 4 presents the results of TEM-EDS analysis. This was performed for F/Base (Fig. 4A) and F2 (Fig. 4B) samples. F/Base sample was consisted of pure zinc oxide nanoparticles and sample F2 was obtained when n GAL : n ZnO ratio was equal to 0.02, the fold of NaOH vs. stoichiometric amount was 2 and the process temperature was 180°C. Pure zinc oxide nanoparticles had spikes-like structure. The particles had bar-like shape with sharp or spear-like ends. The particles were well separated and their size in the smallest dimension was around 100 nm. Zinc oxide nanoparticles modified with galactose were arranged in more chaotic and less organized way. They were in bar-like shape, however the ends of bars were more rounded. In the microphotographs one may observe the organic coating. The size of the smallest dimension was around 50 nm.

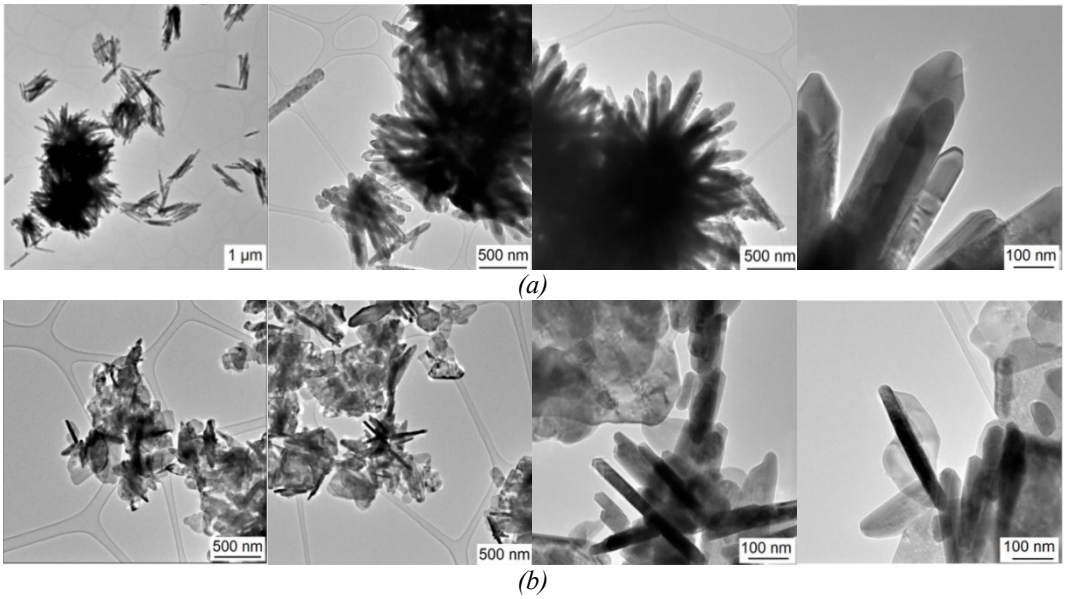

Fig. 4. Results of the TEM analysis: A) F/Base, B) F2.

TEM-EDS analysis revealed that pure zinc oxide nanoparticles were consisted of zinc and oxygen, only (Fig. 5A). The presence of copper results from the apparatus background. TEM-EDS analysis of zinc oxide nanoparticles modified with galactose was also performed (Fig. 5B and 5C). Two different areas were assessed. The first one (Fig. 5B) which was the core of the material was consisted of zinc and oxygen, only. That confirmed that thin bar-like nanoparticles were zinc oxide themselves. The analysis of surrounding coating revealed the presence of carbon which origins from the organic substance, i.e. galactose (Fig. 5C).

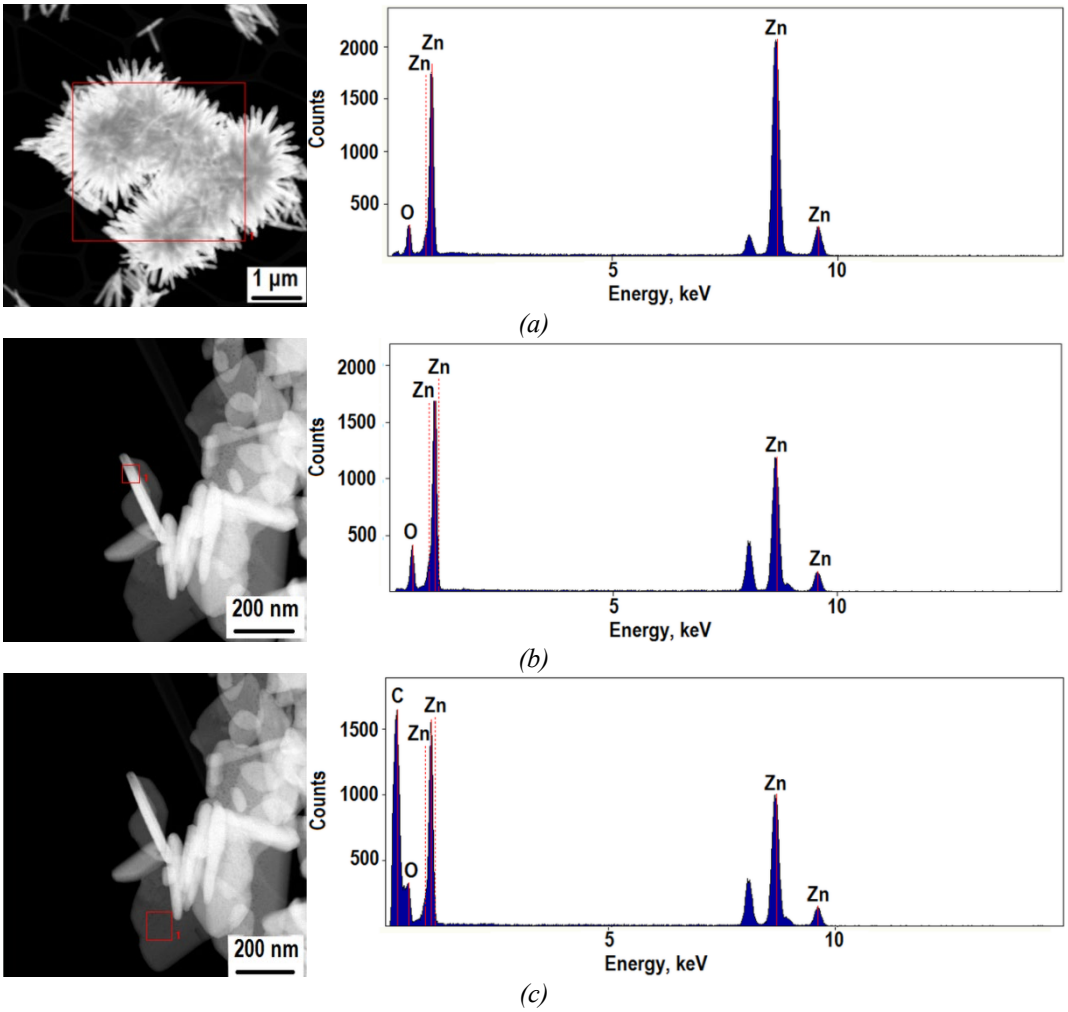

Fig. 5. Results of the TEM-EDS analysis: A) F/Base, B) F2 – core, C) F2 – coating.

In order to measure the size and stability of nanoparticles, DLS technique was applied. Water suspensions of the products at a concentration of 10 ppm was homogenized prior to the size analysis. The stability of the materials was assessed in three different environments. These were deionized water, Ringer fluid and SBF. The size of nanoparticles varied and ranged between 217 and 764 nm (Fig. 6A). Passive cancer therapy uses the anatomical and physiological properties of the neoplastic tissue. The diseased tissue is characterized by increased vascular permeability (leaky network of blood vessels). It was established that the size of the diameter of the fractures is in the range from 100 to 800 nm, while in healthy tissues it is only 2 - 6 nm. The particle size of most anti-cancer drugs is small and does not exceed 10 nm. Therefore, their stand-alone use could cause their penetration into healthy and diseased tissues equally. Therefore, the solution to this problem is to combine molecules of active substances with nanocarriers whose size would be in the range from 50 to 800 nm. As a result, it can be expected that the penetration of the antitumor substance into the structure of the healthy tissue will be limited or eliminated. Concerning the size values obtained by DLS technique, it may be concluded that the prepared modified zinc oxide nanoparticles have satisfactory size since all particles are within the assumed range (50 – 800 nm) (purple line in the Figure 6A). However one should be critical about this technique. This is due to the fact that the primary result of the DLS technique is the particle size distribution by intensity. The light intensity signal is proportional to the sixth power of the particle size. The DLS method is therefore very sensitive to the presence of aggregates and large particles. The intensity distribution is also recalculated using the Mie theory which assumes that the particles are spherical in shape. Therefore, the DLS results may give a false idea of the actual particle size. The analysis of the

nanoparticles stability in different environments provided that the suspensions are stable since in almost all cases the value of electrokinetic potential was greater than 20 nm (Fig. 6B).

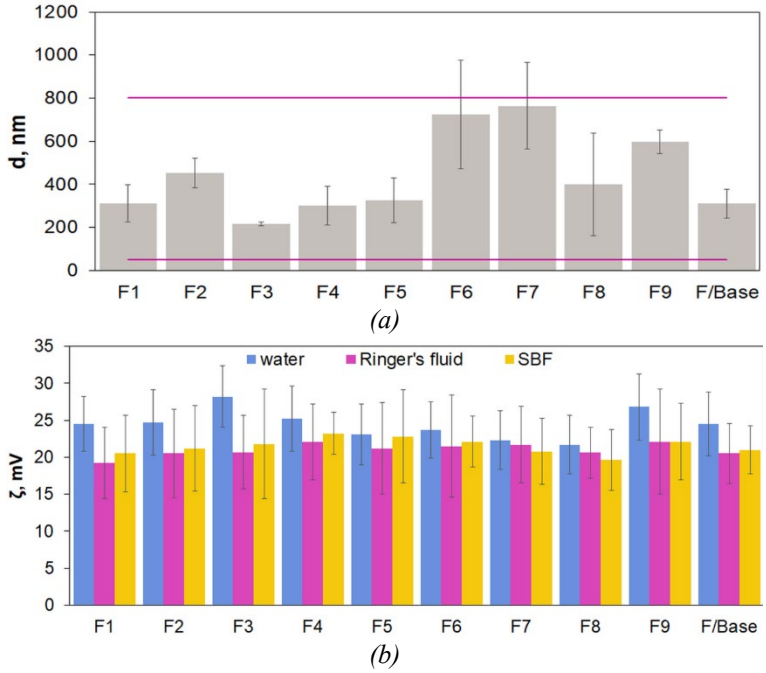

Fig. 6. Results of DLS analysis: A) average size, B) electrokinetic potential, zeta.

3.1. In Vitro Cell viability assay

Figure 6 presents the results of *in vitro* cell viability analysis. The dependence of cytotoxicity on the suspension concentration is presented in Figure 7A. One may observe that in all cases of different concentration of applied nanocarrier the cytotoxicity against CHO cells is reduced comparing to the reference samples (not modified zinc oxide nanoparticles). It has been confirmed that due to the fact that zinc oxide is modified by the presence of galactose on their surface, the cytotoxicity against normal cells has been inhibited. This is extremely desired result which is in line with the preliminary assumptions according to which the galactose inhibits the releasing of zinc which may cause toxic effect by enhancing ROS generation. What is more, the results of the dependence of cells proliferation on the applied concentration show that comparing to the reference materials, in all tested cases the modified zinc oxide nanoparticles favoured the development of the cells (Fig. 7B). It confirms the fact that the produced materials have no harmful effect on the normal cells. Figures 7 C and D present concentration dependent cytotoxicity and proliferation of obtained nanoparticles in CHO cells. One may notice that the higher concentration of modified zinc oxide nanoparticles causes greater cytotoxic effect and favours development of CHO cells to a lesser extent. This proves that the contact of any drug carrier with normal cells is not inert for them, however the contact with modified zinc oxide nanoparticles is still safer than with pure zinc oxide nanoparticles.

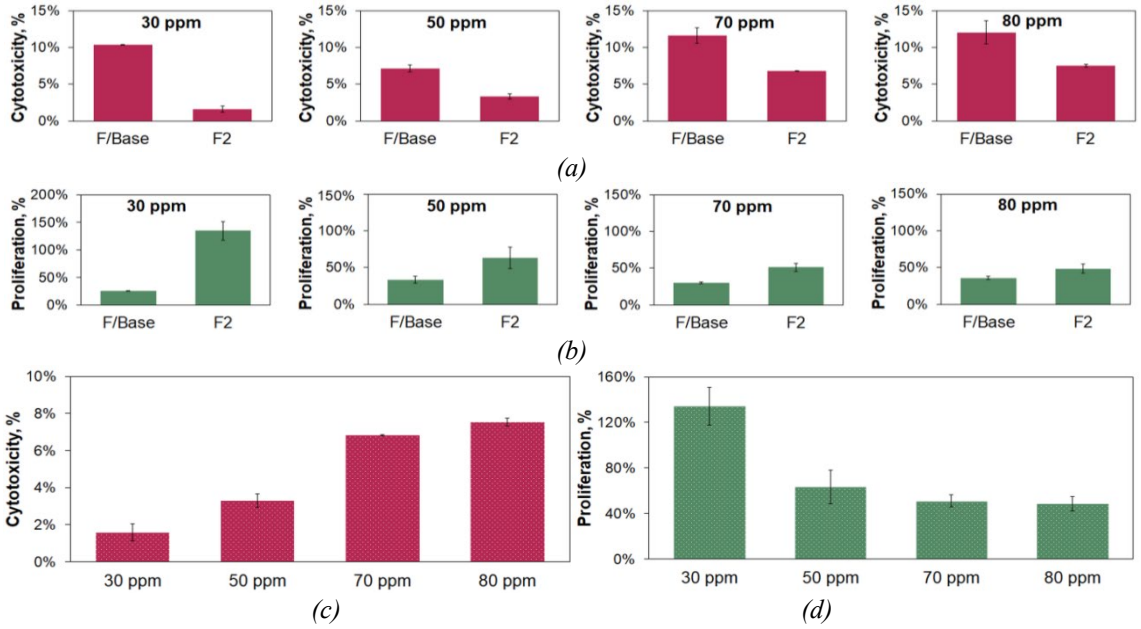

Fig. 7. A) Results of cytotoxicity analysis, B) Results of proliferation analysis C) Concentration dependent cytotoxicity of obtained nanoparticles in CHO cells, D) Concentration dependent proliferation of obtained nanoparticles in CHO cells.

4. Conclusion

Concerning the results it may be concluded that all proposed values of process parameters lead to obtaining stable zinc oxide nanoparticles modified with galactose. It has been confirmed that modified zinc oxide nanoparticles are less cytotoxic to Chinese hamster ovarian cells than pure zinc oxide. What is more the modified nanoparticles favour proliferation of normal cells which is also a desired effect.

Acknowledgements

This work is a part of the project "A method of producing non-toxic carriers of active substances based on nanomaterials," supported by the National Centre for Research and Development, Poland under the agreement LIDER/20/0080/L-9/17/NCBR/2018.

References

[1] J. Jeevanandam, A. Barhoum, Y. S. Chan, A. Dufresne, M. K. Danquah, Beilstein J Nanotechnol 9:1050-1074. (2018); https://doi.org/10.3762/bjnano.9.98

[2] A. Sirelkhatim, S. Mahmud, A. Seeni, N. H. Mohamad Kaus, L. C. Ann, S. K. Mohd Bakhori, H. Hasan, E. Mohamad, Nano-Micro Lett 7, 219 (2015); https://doi.org/10.1007/s40820-015-0040-x

[3] S. Mourdikoudis, R. M. Pallares, N. T. K. Thanh, Nanoscale 10, 12871 (2018); https://doi.org/10.1039/C8NR02278J

[4] R. Rbdel-Karim, Y. Reda, A. Abdel-Fattah, J Electrochem Soc 167, 037554 (2020); https://doi.org/10.1149/1945-7111/ab67aa

[5] P. N. Navya, H. K. Daima Nano Converg 3, 1 (2016); https://doi.org/10.1186/s40580-016-0064-z

[6] J. N. Tiwari, R. N. Tiwari, K. S. Kim, Prog Mater Sci 57, 724 (2012);

https://doi.org/10.1016/j.pmatsci.2011.08.003
[7] M. Subhan, K. Choudhury, N. Neogi, Nanomanufacturing 1, 75 (2021); https://doi.org/10.3390/nanomanufacturing1020008
[8] A. O. Adeola, O. Fapohunda, A. T. Jimoh, T. I. Toluwaloju, A. O. Ige, A. C. Ogunyele, African J Biotechnol 18, 946 (2019); https://doi.org/10.5897/AJB2019.16812
[9] H. Jahangirian, E. Ghasemian Lemraski, T. J. Webster, R. Rafiee-Moghaddam, Y. Abdollahi, A Int J Nanomedicine 12, 2957 (2017); https://doi.org/10.2147/IJN.S127683
[10] Z. X. Yuan, Z. Shang, J. Gu, L. He, Future Med Chem 11, 2237 (2019); https://doi.org/10.4155/fmc-2019-0152
[11] Z. Mahdavi, H. Rezvani, M. Keshavarz Moraveji, RSC Advances 10, 18280 (2020); https://doi.org/10.1039/D0RA01032D
[12] Y. Yao, Y. Zhou, L. Liu, Y. Xu, Q. Chen, Y. Wang, S. Wu, Y. Deng, J. Zhang, A. Shao, Front Mol Biosci 7, 193 (2020); https://doi.org/10.3389/fmolb.2020.00193
[13] A. A. Yetisgin, S. Cetinel, M. Zuvin, A. Kosar, O. Kutlu, Molecules 25, 2193 (2020); https://doi.org/10.3390/molecules25092193
[14] D. Chenthamara, S. Subramaniam, S. G. Ramakrishnan, S. Krishnaswamy, M. M. Essa, F. H. Lin, W. Qoronfleh, Biomater Res 23, 20 (2019); https://doi.org/10.1186/s40824-019-0166-x
[15] V. Kumar Khanna, ISRN Pharmacol 2012, 571394 (2012); https://doi.org/10.5402/2012/571394
[16] M. J. Mitchell, M. M. Billingsley, R. M. Haley, M. E. Wechsler, N. A. Peppas, R. Langer, Nat Rev Drug Discov 20, 101 (2021); https://doi.org/10.1038/s41573-020-0090-8
[17] L. Houdaihed, J. C. Evans, C. Allen, Pharm Res 37, 39 (2020); https://doi.org/10.1007/s11095-019-2684-6
[18] S. Muro, Biomimetics 3, 19 (2018); https://doi.org/10.3390/biomimetics3030019
[19] O. S. Thomas, W. Weber, Front Bioeng Biotechnol 7, 415 (2019); https://doi.org/10.3389/fbioe.2019.00415
[20] G. Bisht, S. Rayamajhi, Nanobiomedicine 3, 9 (2016); https://doi.org/10.5772/63437
[21] M. P. Nikolova, M. S. Chavali, Biomimetics 5, 27 (2020); https://doi.org/10.3390/biomimetics5020027
[22] O. Długosz, K. Szostak, A. Staroń, J. Pulit-Prociak, M. Banach M, Materials 13, 279 (2020); https://doi.org/10.3390/ma13020279
[23] P. Wu, J. Han, Y. Gong, C. Liu, H. Yu, N. Xie, Pharmaceutics 14, 1990 (2022); https://doi.org/10.3390/pharmaceutics14101990
[24] G. Sanità, B. Carrese, A. Lamberti, Front Mol Biosci 7, 587012 (2020); https://doi.org/10.3389/fmolb.2020.587012
[25] N. Lagopati, P. V. Kitsiou, A. I. Kontos, P. Venieratos, E. Kotsopoulou, A. G. Kontos, D. D. Dionysiou, S. Pispas, E. C. Tsilibary, P. Falaras, J. Photochem Photobiol A Chem 214, 215 (2010); https://doi.org/10.1016/j.jphotochem.2010.06.031
[26] P. Sadhukhan, M. Kundu, S. Chatterjee, N. Ghosh, P. Manna, J. Das, P. C. Sil, Mater Sci Eng C 100, 129 (2019); https://doi.org/10.1016/j.msec.2019.02.096
[27] M. J. Akhtar, M. Ahamed, S. Kumar, M. A, Majeed Khan, J. Ahmad, S. A. Alrokayan, Int J Nanomedicine 7, 845 (2012)
[28] H. Mirzaei, M. Darroudi, Ceram Int 43, 907 (2017); https://doi.org/10.1016/j.ceramint.2016.10.051
[29] J. W. Rasmussen, E. Martinez, P. Louka, D. G. Wingett, Expert Opin Drug Deliv 7, 1063 (2010); https://doi.org/10.1517/17425247.2010.502560
[30] L. Wang, J. Mao, G. H. Zhang, M. J. Tu, World J Gastroenterol 13, 4011 (2007); https://doi.org/10.3748/wjg.v13.i46.6269